Chapter 5

Identification and Results

In this chapter, each of the ARTISAN wrist joint system components is identified by employing a variety of methods. The combined open loop system is derived and the characteristics of the system discussed. Finally, the results of the control design are presented along with a simulation of the closed loop system demonstrating the torque loop's potential performance.

5.1   Identification of Components

Different methods of identification were used for each of the different components of the ARTISAN link torque loop. For each component, the identification method employed and the resulting pole/zero plot are provided for greater clarification.

5.1.1   Motor and Amplifier

Using the assumption that Inland Motor properly identified the system equations for the BDA Current Amplifier and the RBE(H) Motor, identification of the motor and amplifier system became a simple substitution of parameters into the system

equation provided in Section 2.2.1. Using Equation (2.1) and Table 2-2, the realization of the motor and amplifier is shown in Equation (5.1).

$$\frac{i_m}{v_c} = \frac{810(s + 4263.8)}{s^2 + 1507.2s + 2.4671377e6} \tag{5.1}$$

The resulting pole/zero map of the system is shown in Figure 5-1.
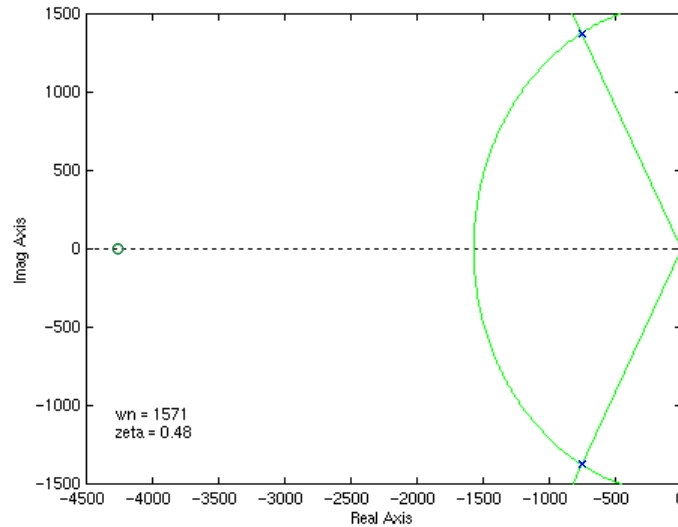
Figure 5-1: Motor and Amplifier Poles and Zero

5.1.2   Mechanical Sensor

In order to identify the characteristics of the mechanical sensor, a known torque source and measurement system are used to create a testbed to measure the response of the mechanical sensor. As shown in Figure 5-2, a torque is created by the BDA Current Amplifier and RBE(H) Motor and applied to the sensor through the gearing mechanism. The sensor deflection is sensed by a pair of LVDTs and the Analog Devices 2S54 LVDT-to-Digital Converter for which the system response has been identified.
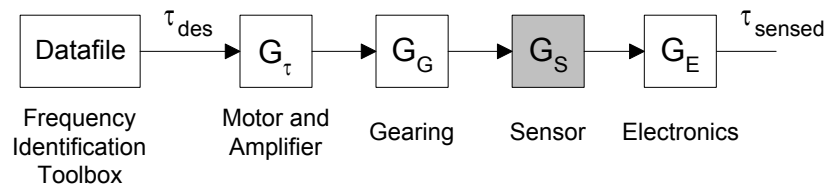
Figure 5-2: System Setup for Mechanical Sensor Identification

The torque command is created using a band-limited multi-sine, generated with Professor Istvan Kollar's Frequency Identification Toolbox in MATLAB^{TM}. The multi-sine is an excitation signal comprised of a range of sinusoids selected at certain frequencies and amplitudes to excite the unknown system modes. This method is preferable to sweep-sine or one-at-a-time frequency identification methods since it provides a single excitation signal containing a range of frequencies without causing major physical damage due to prolonged identification commands.

Once the data is collected from the test, the Frequency Identification Toolbox creates an approximation of the transfer function based on the assumed structure for the entire system. The response of the known components - the motor, current amplifier and converter - is then subtracted from the overall response and the remaining transfer function is identified as the mechanical sensor.

Numerous tests identified the mechanical sensor transfer function as shown in Equation (5.2). The resonant modes of the sensor are lightly damped, as discussed in Section 3.2.2, which leads to the assumption that the damping factors do not significantly impact the mechanical response.

$$\frac{\tau_s}{\tau_m} = \frac{1.9564e6}{s^2 + 159.32s + 1.4492e5} \tag{5.2}$$

The corresponding pole/zero map for the sensor is shown in Figure 5-3.
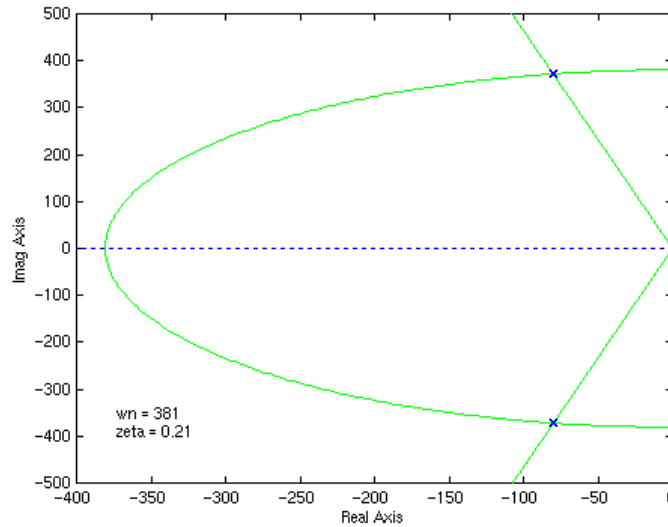
Figure 5-3: Mechanical Sensor Poles

5.1.3 Sensor Electronics

As discussed in Appendix C, the single pole structure for the Loop Compensator is selected for the AD2S93 for its fast rise time and low overshoot characteristics. To derive a transfer function for the resulting system, the Least Squares method is used to minimize the difference between the actual and the theoretical step response. The resulting transfer function is a third order system with two dominant complex roots with heavy damping (zeta = 0.75) and a third pole with the real part ten times greater than the complex roots.

$$\frac{\Delta x_d}{\Delta x_v} = \frac{2.456e12}{s^3 + 1.039e5s^2 + 7.511e8s + 2.456e12} \tag{5.3}$$

The step response of the theoretical system closely follows the actual step response as shown in Figure 5-4. The resulting pole/zero map is shown in Figure 5-5, at a scale which does not show the high frequency pole.
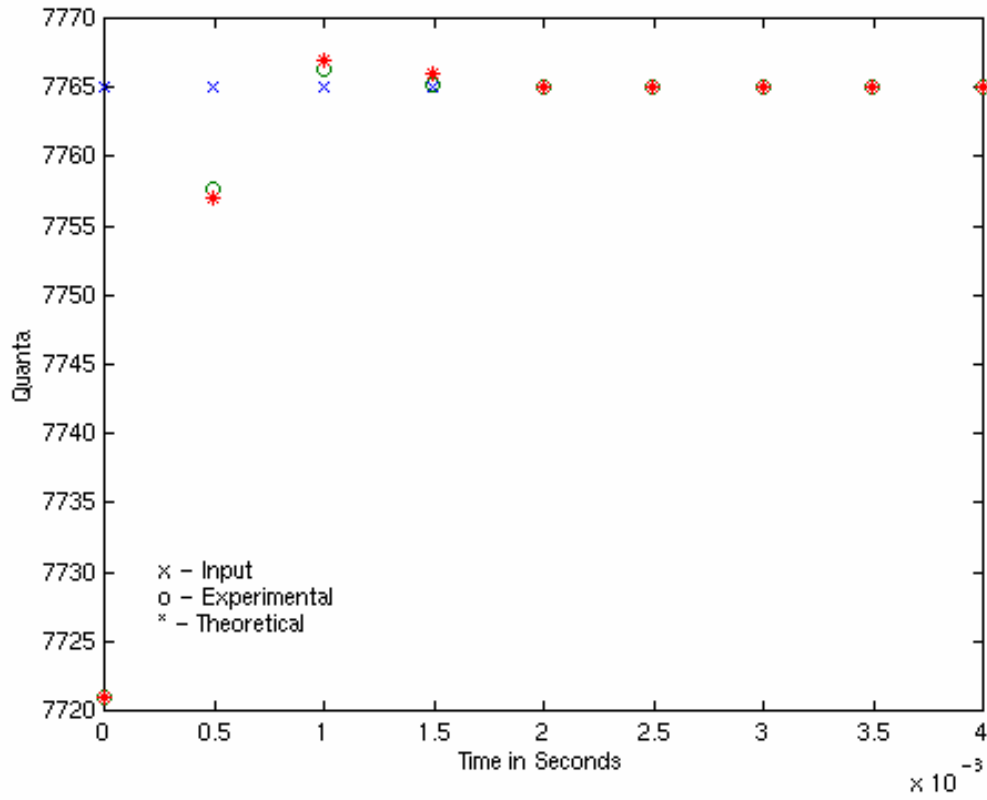
Figure 5-4: Experimental and Theoretical Step Responses of AD2S93
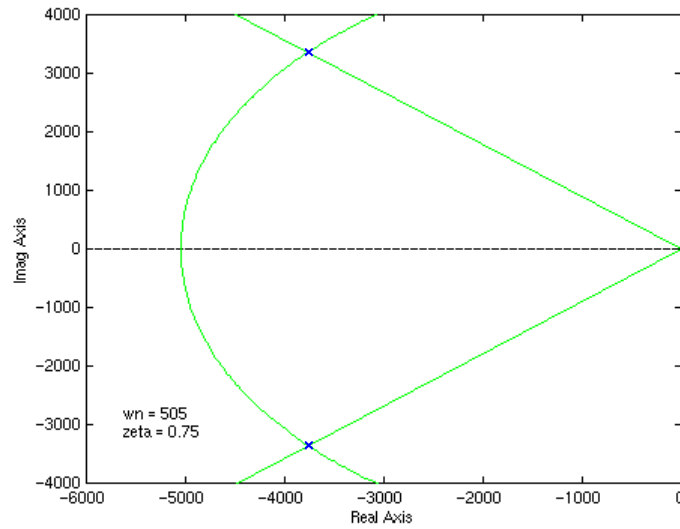
Figure 5-5: Dominant Poles of Sensor Electronics

5.1.4   Complete Open Loop System

The pole zero map in Figure 5-6 combines all three systems, resulting in a seventh-order system with a single zero contributed by the motor/amplifier system. The shaded areas indicate the separate dynamic contributions of each of the system components.
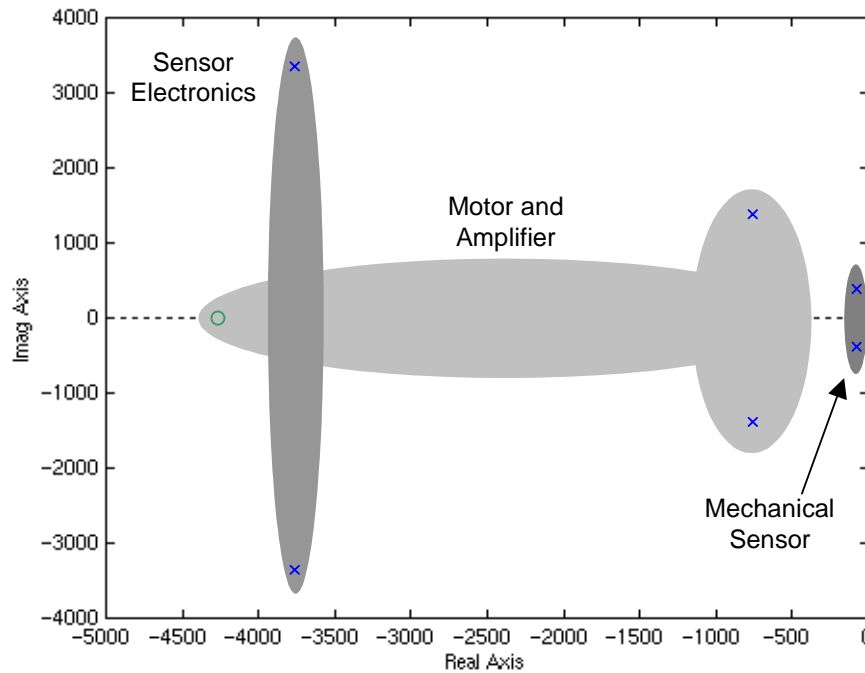
Figure 5-6: Complete Pole/Zero Map of Open Loop System

The Bode Plot of the open loop system without gain normalization in Figure 5-7 shows a gain margin of -22.6dB and no phase margin.
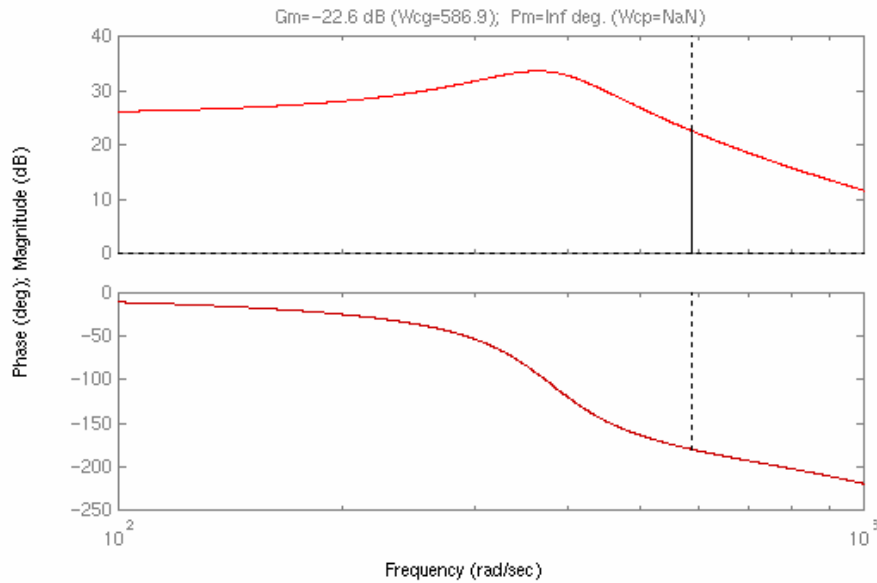
Figure 5-7: Bode Plot of Complete Open Loop System

With gain normalization, the gain margin becomes 3dB and the phase margin is a 10.7 degrees, as shown in Figure 5-8.
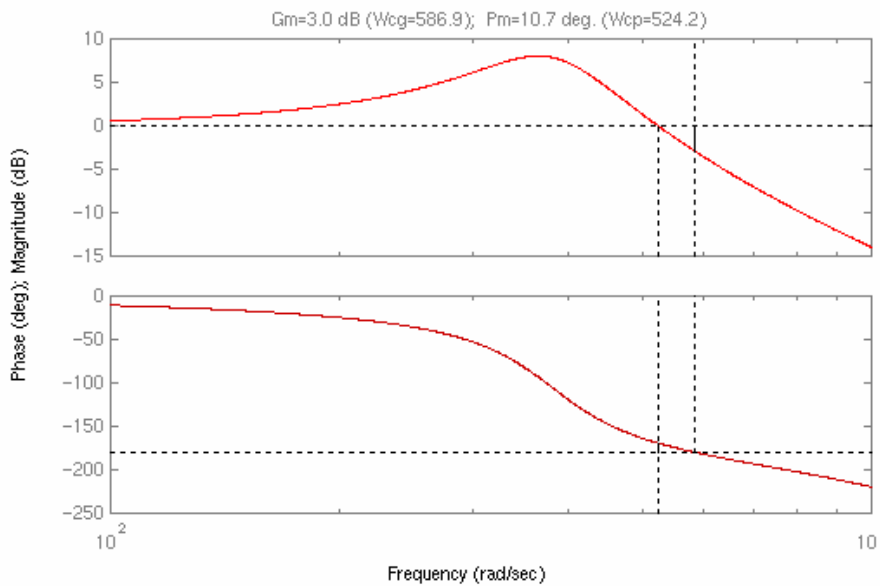
Figure 5-8: Bode Plot of Normalized Open Loop System

5.2   Controller Design

Once the complete open loop system has been identified, the symmetric root locus of the system is created to determine the optimal pole placement using the LQR performance index. The symmetric root locus takes the transfer function of the open loop system $G_0(s)$:

$$G_0(s) = \frac{N(s)}{D(s)} \qquad (5.4)$$

The poles of the root locus characteristic equation are then derived using the following equation:

$$1 + \rho \frac{N(s)N(-s)}{D(s)D(-s)} = 0 \qquad (5.5)$$

where ρ is the weighting factor defined in Section 4.4.

Once the symmetric root locus is created, the time domain specifications from Table 4-2 are used to provide a region in the s-plane for the closed loop poles to reside.   As shown in Figure 5-9, when the weighting factor is increased, the mechanical sensor poles enter the desired (unshaded) region, but the motor and amplifier poles remain outside the desired closed loop region. In addition, the motor and amplifier poles become the more dominant poles, forcing the response of the closed loop system to follow their characteristics.
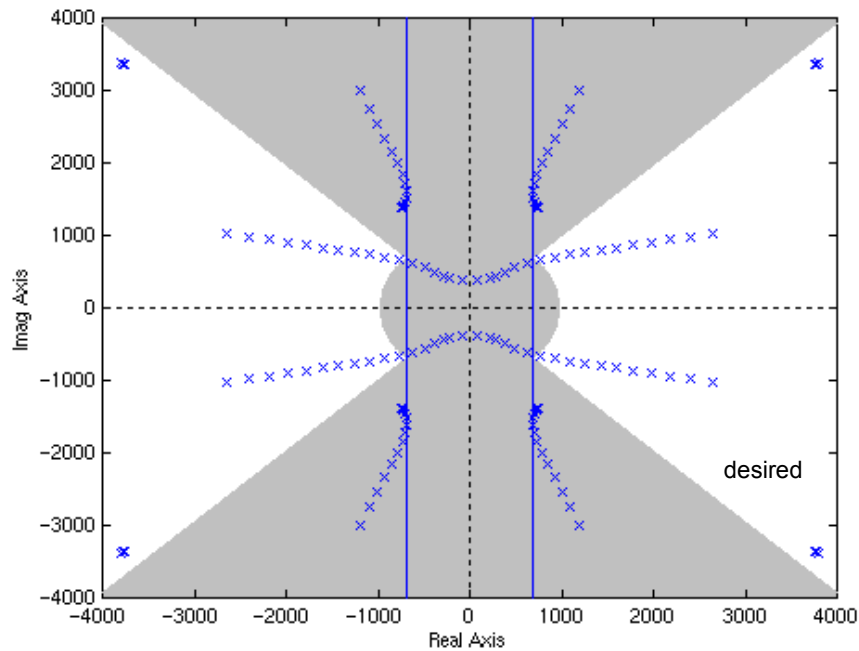
Figure 5-9: Symmetric Root Locus with Desired Region in white

With the motor and amplifier poles becoming the dominant poles as the weighting factor is increased, the choice of ρ becomes a tradeoff between overshoot and bandwidth. As shown in Figures 5-10 and 5-11, when the weighting factor is increased, the rise time of the closed loop response improves while the overshoot degrades. To achieve the improved rise time, additional control effort is required. From Figure 5-12, a moderate value of $\rho = 8N$ was selected.
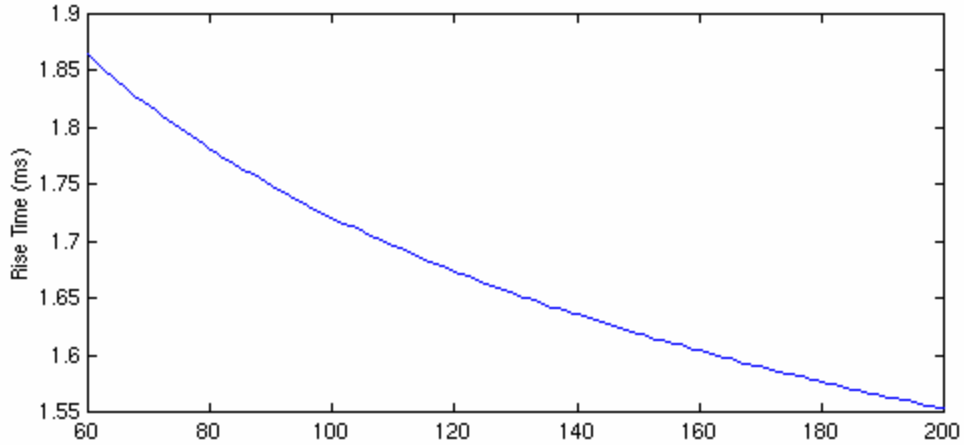
Figure 5-10: Rise Time with respect to Weighting Factor
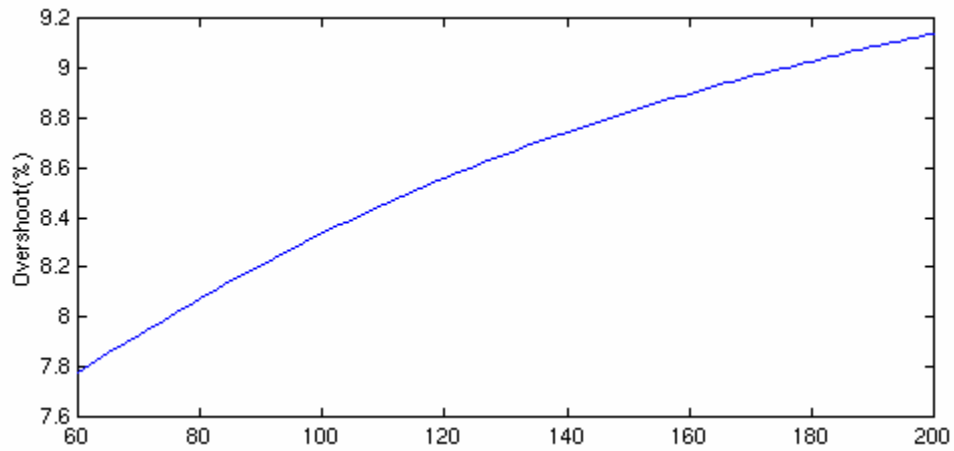
Figure 5-10: Overshoot with respect to Weighting Factor
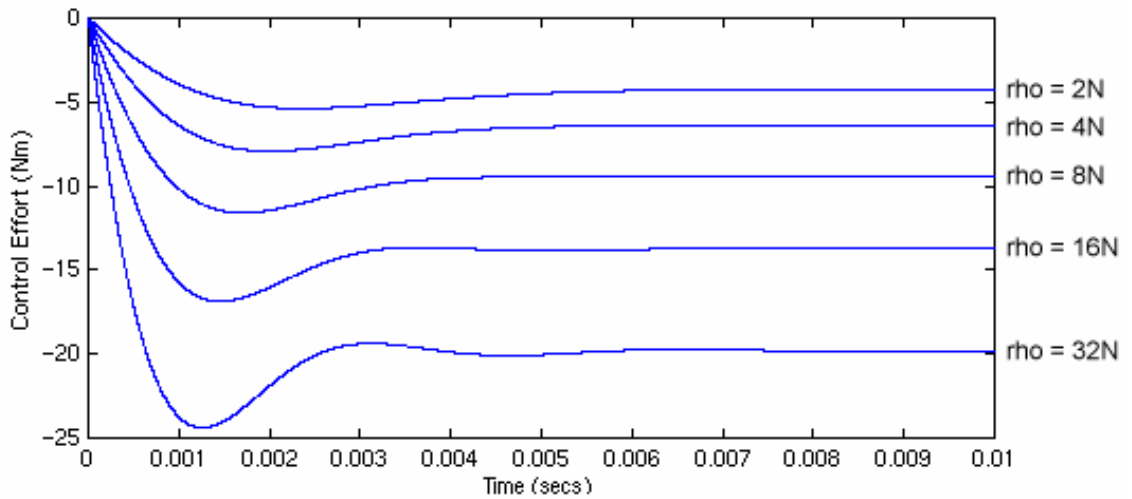
Figure 5-12: Control Effort with respect to Weighting Factor

Based on the selected ρ value, the LQR state feedback gain matrix, K, is defined:

$$K = \begin{bmatrix} 97.1657 & 315.4632 & 182.6478 & 208.509 & 100.3374 & 123.053 & 219.4144 \end{bmatrix}$$

which results in the following closed loop poles for the torque loop:

$$\text{eig(A-BK)} = \begin{bmatrix} -96416.6837 \\ -3762.9152 + j3363.5369 \\ -3762.9152 - j3363.5369 \\ -684.1355 + j1516.457 \\ -684.1355 - j1516.457 \\ -926.3867 + j700.3168 \\ -926.3867 - j700.3168 \end{bmatrix}.$$

Once the state feedback gains are selected, a set of state estimator gains are selected that maximizes the ratio between the poles of the estimator and the closed loop poles of the state-feedback system. Based on this criterion, the state estimator gain matrix, L, is defined:

$$L^T = \begin{bmatrix} 285.5232 & 3758.515 & 4849.932 & 26333.619 & 40625.922 & 7372.207 & 171.646 \end{bmatrix}$$

These estimator gains result in the following estimator poles and a ratio of 4.1322 between the slowest estimator root and the slowest torque loop root.

$$\text{eig(A-LC)} = \begin{bmatrix} -96416.6837 \\ -1986.3928 + j5816.7488 \\ -1986.3928 - j5816.7488 \\ -4949.4552 + j4031.6791 \\ -4949.4552 - j4031.6791 \\ -4798.7956 + j0.3168 \\ -4798.7956 - j0.3168 \end{bmatrix}$$

5.2.1   Simulation

The system equations for the ARTISAN wrist joint are simulated with the state feedback gains using states generated from the state estimator using SIMULINK. As shown in Figure 5-13, the step response of the simulated closed loop system results in a rise time of 1.703 milliseconds with an overshoot of 8.3%. Even though these time domain specifications do not exactly meet the desired characteristics, they represent an optimal tradeoff between bandwidth, overshoot and control effort limitations for this system.
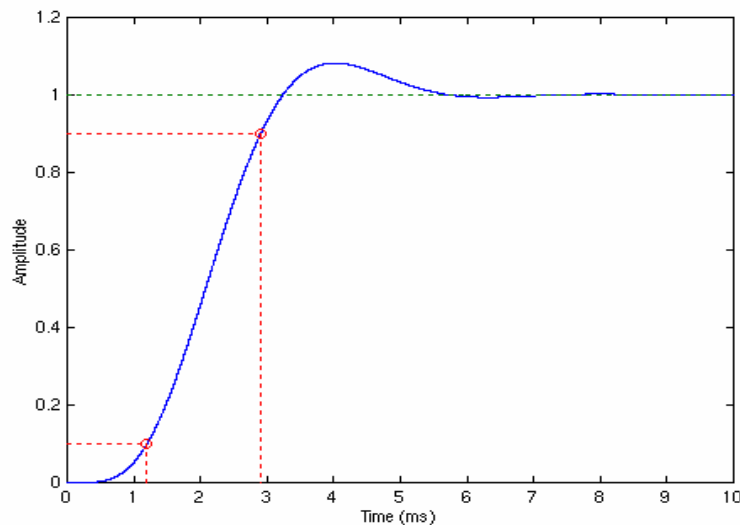
Figure 5-13: Step Response of Closed Loop System

The open-loop Bode Plot in Figure 5-14 shows several improvements. The gain margin is improved to 8dB, the phase margin is increased to 42.7 degrees and the final bandwidth to 216 Hz through the use of the LQR/LQE compensation.
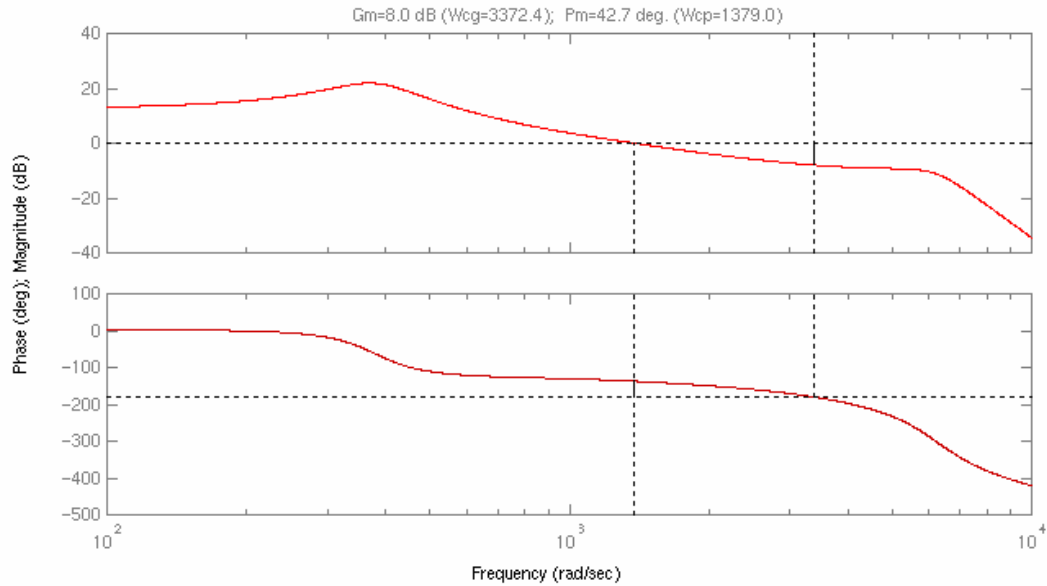
Figure 5-14: Bode Plot of Open Loop System with Compensation

5.3   Summary

The resulting closed loop system for the ARTISAN wrist joint torque loop provides much faster response than the open loop system shown in Figure 5-15. The final closed loop response is a tradeoff between control effort and the desired time domain characteristics.
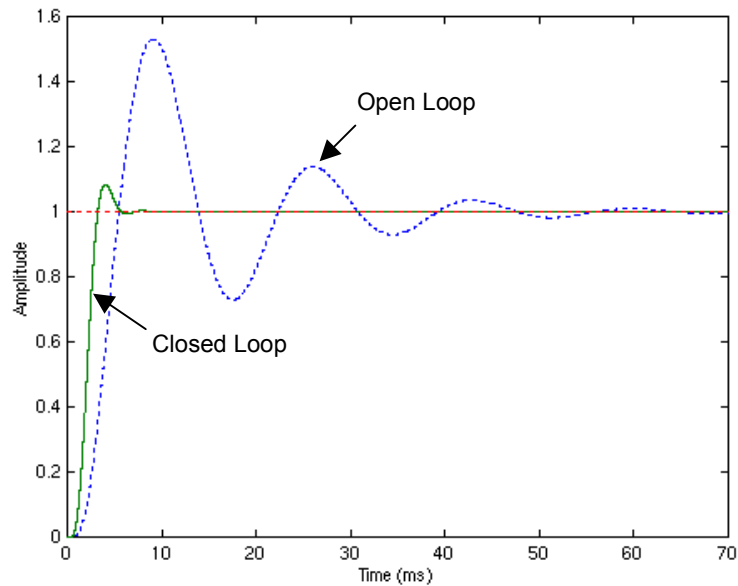
Figure 5-15: Open and Closed Loop Step Responses

Due to the presence of the motor and amplifier poles, the desired time domain specifications enumerated in Section 4.1 were not attainable using the LQR/LQE method for controller design. The resulting bandwidth of 216.7 Hz, as shown in Figure 5-16, means that when designing the outer kinematic loop compensation, the dynamic characteristics for the torque loop can not be ignored and must be taken into account.
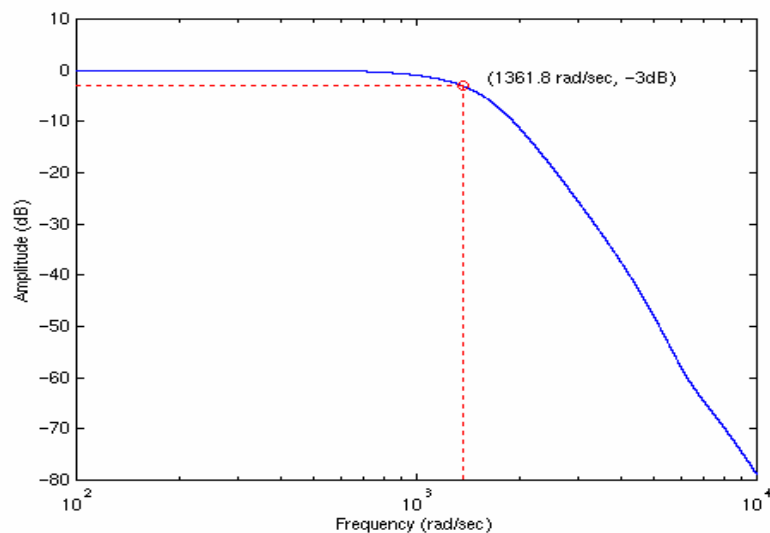
Figure 5-16: Closed Loop Frequency Response with Corner Frequency Labeled